Slow-light solitons in two-level media generated by evanescent fields

Jérôme Leon
Laboratoire de Physique Théorique et Astroparticules CNRS-IN2P3-UMR5207, Université Montpellier 2, 34095 Montpellier, France
(Received 12 March 2007; revised manuscript received 10 April 2007; published 12 June 2007)

Coupling a two-level medium, described by the Maxwell-Bloch (MB) equations, to an external cavity mode results in a prescribed boundary value for the electric field that can be tuned to the forbidden band gap of the medium. It is shown that there exists a threshold of energy density flux above which a solitonlike light pulse is generated and propagates in the medium at a fraction of the light velocity. When the driving frequency becomes close to the band gap edge, where the group velocity vanishes, the MB equations tend to the nonlinear Schrödinger equation which furnishes the theoretical ground to understand soliton generation by evanescent fields as a manifestation of nonlinear supratransmission, produced by an instability of the evanescent wave. Moreover, the propagation at a fraction of light velocity is shown to result from a continuous periodic exchange between polarization (electromagnetic energy) and population (density of atoms in the excited level). The process is demonstrated to occur at twice the internal frequency of the generated gap soliton. Last, when the medium spatial extension is of the order of the soliton dimension, an optical bistability is shown to occur at the supratransmission threshold allowing for different output intensities corresponding to a given input value.

DOI: 10.1103/PhysRevA.75.063811 PACS number(s): 42.65.Tg, 42.50.Gy, 42.65.Re

I. INTRODUCTION

The propagation of an electromagnetic field in a dielectric medium is one of the main basic problems founding the field of interaction of radiation with matter [1]. When the medium can be treated as a two-level system, as, e.g., an atomic gas for a given frequency range of the electromagnetic field, the governing equations in the dipolar approximation result to be the Maxwell-Bloch system (MB) which couples the evolution of the electric field (Maxwell equations) to the polarization oscillations and population density variations (Bloch equations) [2].

In the isotropic case, as for an atomic vapor, following the notations of [3], the MB equations for the three-vectors **E** (electric field) and **P** (polarization source term: $\mathbf{D}=\epsilon\mathbf{E}+\mathbf{P}$) can be written

$$\nabla\times\nabla\times\mathbf{E}+\frac{\eta^2}{c^2}\frac{\partial^2\mathbf{E}}{\partial t^2}+\frac{\eta}{c}\mathcal{A}\frac{\partial\mathbf{E}}{\partial t}=-\mu_0\frac{\partial^2\mathbf{P}}{\partial t^2},$$

$$\frac{\partial^2\mathbf{P}}{\partial t^2}+\frac{2}{T_2}\frac{\partial\mathbf{P}}{\partial t}+\Omega^2\mathbf{P}=-\kappa N\mathbf{E},$$

$$\frac{\partial N}{\partial t}+\frac{1}{T_1}(N-N_{eq})=\frac{2}{\hbar\Omega}\mathbf{E}\cdot\frac{\partial\mathbf{P}}{\partial t},\tag{1}$$

where N is the real-valued inversion of population density (the difference of population between excited and fundamental levels) of equilibrium value N_{eq}. The parameter Ω is the dipole transition frequency, $\eta=\sqrt{\epsilon/\epsilon_0}$ is the optical index, and the fundamental *coupling constant*

$$\kappa=\frac{2\Omega}{\hbar}\left(\frac{\eta^2+2}{3}\right)^2\frac{1}{3}\langle|\mu_{12}|^2\rangle\tag{2}$$

is related to the electric dipole moment μ_{12} (the average is taken over the orientations). The coefficient $(\eta^2+2)/3$ is the Lorentz local field correction factor. The damping terms result from the attenuation $\mathcal{A}$ of the electric field and the relaxation times T_1 and T_2.

The parameter κ is the fundamental coupling constant as the interaction dissapears at $\kappa=0$. Thus the intrinsic nonlinear nature of MB is entirely *mediated by the atoms*: it is the time variation of the density N that induces nonlinearity with an intensity related to the coupling constant κ.

In the case of a *weak coupling*, namely for underdense media, nonlinearity allows for *self-induced transparency* (SIT) of a light pulse whose peak frequency is tuned to the resonant value Ω, when a linear theory would predict total absorption [4]. SIT has been then largely studied [5], and the model (in the slowly varying envelope approximation) results to be integrable [6] and to have the *mathematical* property of transparency: any fired pulse having an area above a threshold evolves to a soliton, plus an asymptotically vanishing background [7]. The point is that within the integrable SIT model, the incident pulse (boundary datum) maps to an *initial value problem* on the infinite time line for which the inverse spectral transform machinery provides useful theorems.

Away from the resonance, and also for dense media, the question of the propagation of laser pulses in a two-level medium has motivated a huge quantity of works. A widely used approach consists in modeling the dynamical nonlinear properties of pulse propagation by an approximate envelope equation that selects propagation in one direction, the *reduced Maxwell-Bloch system* which has the nice property of being integrable [8,9], also when detuning and permanent dipole are included [10]. As a consequence the properties of the *gap soliton*, such as pulse reshaping, pulse slowing, pulse-pulse interactions, are fairly well understood, more especially as the reduced MB system possesses explicit N-soliton solutions [11]. Others interesting features include pulse velocity selection [12]. However, unlike the SIT model, the reduced MB system happens to be integrable for an *initial pulse profile* which makes it difficult to relate to the interesting physical problem, namely the evolution of an incident light pulse.

In order to improve the description of a more realistic physical situation, the reduced MB equation was then replaced by the *coupled-mode Maxwell-Bloch* system where the electric field envelope contains both right-going and left-going slowly varying componants [13]. Here, an incident laser pulse is translated on the model by an assumed pulse-shaped *boundary condition* for the right-going envelope (naturally associated with a left-going envelope that vanishes on the other end of the medium). As usual in such a representation of a scattering problem, the adequation of the model to the physical situation is a very difficult question often left apart. Still, the approach produces interesting results, as, e.g., the proof of existence of gap 2π pulses in the presence of inhomogeneous broadening [14] and their stability [15], the discovery of *optical zoomerons* [16], and the demonstration of the possibility of "*storage of ultrashort optical pulses*" [17] demonstrated by numerical simulations of the coupled-mode MB system associated to such a boundary value problem. This storage can moreover be externally managed to release the stored pulse and thus create a "*gap soliton memory*" with a two-level medium [18].

The coupled-mode approach has also been applied to understand the properties of *resonantly absorbing Bragg reflectors* introduced in [19] and further studied in [20,21], which consist in a periodic array of dielectric films separated by layers of a two-level medium. Very recently, the coupled-mode MB system has been used to model "*plasmonic Bragg gratings*" in nanocomposite materials where a dielectric is imbedded in a periodic structure of thin films made of metallic nanoparticules [22].

Turning back to the original full MB system, the proper mechanism of *soliton generation* by means of light pulse scattering still remains an open question. In particular, a laser pulse having a peak frequency belonging to the gap, would essentially be reflected, and would not generate a gap soliton. Moreover, numerical simulations have shown that the localized gap structures (unlike true solitons) experience energy exchange during interaction [23]. Hence gap-solitary waves result mathematically from an *initial condition* in the MB equations, which is hardly realizable in experiments, although quite interesting, e.g., to form "*optical subcycle pulses*" [24].

We propose here to couple a two-level medium to a resonant cavity tuned such as to generate a standing wave whose frequency belongs to the forbidden band gap of the medium. Indeed, for an attenuator ($N_{eq}<0$) in the strong coupling case, the linear dispersion relation of the undamped system (1) shows a forbidden band gap between the two dispersion branches. In the stop gap frequency range, the two-level medium then acts as a Bragg mirror allowing to conceive a cavity as represented by the scheme of Fig. 1.

The net result of the external driving by a cavity mode (of angular frequency ω_b) is to produce, by continuity conditions for the electric field parallel component, a boundary value datum for the set of equations (1) which we may write

$$\mathbf{E}|_{z=0} = \mathbf{A}\cos(\omega_b t), \tag{3}$$

when the electric field $\mathbf{E}(\mathbf{r},t)$ is linearly polarized in the tranverse direction (see below). The input flux power density

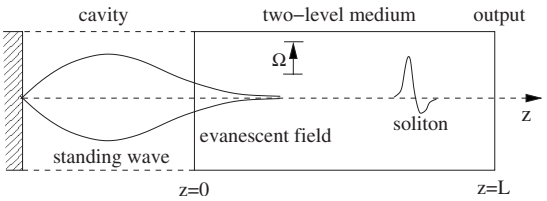

FIG. 1. Scheme of the device that couples a cavity mode whose frequency in the forbidden gap of a two-level medium. The evanescent field in the medium may experience a nonlinear instability that produces a solitonlike propagating pulse.

(proportionnal to $\mathbf{A}^2$) is related both to the energy and the angular frequency ω_b of the electric field stored in the cavity. In particular it is a parameter that can be externally adjusted.

We demonstrate that there exists a threshold of input flux density above which solitonlike excitations are generated and propagate inside the two-level medium. The mechanism is an instability of the evanescent field [25] allowing energy to be transmitted by the process of *nonlinear supratransmission* [26,27], which results in a soliton train output. Thus the two-level medium pumped at one end by a standing cavity wave inside a stop gap becomes a *soliton gun* which may have important physical applications. Such a process occurs here in the very general MB system by the effect of *extrinsic nonlinearity*, due to coupling of field with medium, as opposed to integrable models with *intrinsic nonlinearity* such as nonlinear Schrödinger [28,29] or sine Gordon [30,31].

One of the interesting aspects of the process is the velocity of the generated soliton like pulse which happens to be a fraction of the light velocity in the medium (typically 10% in our simulations). We will demonstrate that it is a *fully nonlinear effect* contained in the MB system which occurs by a periodic continuous exchange between polarization energy and population of excited level. Moreover, we shall show that the frequency of such an energy exchange comes to be twice the pulse frequency, which will be understood by using the nonlinear Schrödinger limit equation (NLS) obtained in a rigorous asymptotic limit [32]. In particular a rough approximation that would simply neglect higher harmonics (the so-called *rotating wave approximation*) would not allow one to understand this periodic exchange at the origin of slow-light pulses propagation.

Another essentially nonlinear property of the Maxwell-Bloch system submitted to boundary driving is the *optical bistability* that manifests in the existence of solutions with different outputs for a given input and different *history*. This question, interesting for applications to optical switches, memories, or digital amplifiers, is considered in the last section where the process is again understood with help of the NLS limit envelope equation.

II. INITIAL BOUNDARY VALUE PROBLEM

The system (1) is considered in the simplest case of a linearly polarized electromagnetic field propagating in direction z, namely ($\mathbf{e}_x$ is the unit vector),

$$\mathbf{E}(\mathbf{r},t) = \mathbf{e}_x E(z,t) \Rightarrow \mathbf{P}(\mathbf{r},t) = \mathbf{e}_x P(z,t). \tag{4}$$

By defining N_0 as the density of *active atoms*, it is quite useful to define the average energy that can be transferred to the medium by

$$w_0 = \frac{1}{2} N_0 \hbar \Omega. \tag{5}$$

Then we may rescale variables and fields as

$$t' = \Omega t, \quad z' = \frac{\eta}{c} \Omega z, \quad N' = \frac{N}{N_0}, \tag{6}$$

$$E' = E \sqrt{\frac{\epsilon}{w_0}}, \quad P' = \frac{P}{\sqrt{\epsilon w_0}}, \tag{7}$$

and obtain the following dimensionless system

$$E_{tt} - E_{zz} + P_{tt} = -\gamma E_t,$$

$$P_{tt} + P + \alpha N E = -\gamma_2 P_t,$$

$$N_t - E P_t = -\gamma_1 (N - N_{eq}), \tag{8}$$

where from now on we forget the primes. The coupling strength results in a unique fundamental constant α defined as

$$\alpha = \frac{2\mu_0 c^2}{3\eta^2} \langle |\mu_{12}|^2 \rangle \frac{N_0}{\hbar \Omega} \left(\frac{\eta^2 + 2}{3} \right)^2, \tag{9}$$

and by the normalization of the population inversion density ($N \in [-1, 1]$), where $N=-1$ when all the active atoms are in the fundamental state, and $N=1$ when they are all in the excited state. The dimensionless dissipation coefficients are finally defined by

$$\gamma = \frac{c}{\eta} \frac{\mathcal{A}}{\Omega}, \quad \gamma_1 = \frac{1}{\Omega T_1}, \quad \gamma_2 = \frac{2}{\Omega T_2}. \tag{10}$$

The dimensionless *irreducible* constant α characterizes the strength of the nonlinear interaction between field and medium.

In the case of an attenuator when the N_0 atoms are initially in the fundamental state (namely, $N_{eq}=-1$ or with dimensions $N_{eq}=-N_0$), the resulting initial data read

$$E(z,0) = 0, \quad P(z,0) = 0, \quad N(z,0) = -1. \tag{11}$$

The net effect of the presence of the cavity is the boundary driving (3) which becomes here

$$E(0,t) = a \cos(\omega_d t), \tag{12}$$

where, due to the scaling of time (6), the driving angular frequency ω_d is in units of Ω, namely $\omega_b = \omega_d \Omega$. The system of partial differential equations (8) constitutes with the initial-boundary value data equations (11) and (12), a well-posed problem if it is completed with a boundary value at the output end of the two-level medium. When outside the two-level medium ($z > L$), the electric field is assumed to be constant, the continuity of the magnetic component furnishes the boundary datum

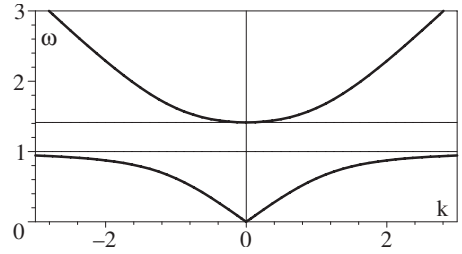

FIG. 2. The two branches of the dispersion relation for the dimensionless system (8) in the case $\alpha=1$. The stop gap is $[1, \omega_0]$.

$$E_z(L,t) = 0. \tag{13}$$

Actually such a boundary condition is not determinant for long lengths L (a few times the typical soliton extension) where one is only interested in the gap soliton formation.

The linear dispersion relation of system (8) is obtained by assuming $N=-1$, $E=E_0 \exp[i(kz-\omega t)]$, $P=P_0 \exp[i(kz-\omega t)]$, and by discarding the coupling nonlinear terms. It reads

$$(\omega^2 - k^2)(\omega^2 - 1) - \alpha \omega^2 = 0, \tag{14}$$

which furnishes the two branches and the stop gap illustrated on Fig. 2. The upper edge of the stop gap defines the frequency

$$\omega_0^2 = 1 + \alpha, \tag{15}$$

for which $k=0$ and $v_g = d\omega/dk = 0$.

The problem we are interested in is thus the behavior of the two-level medium under a boundary driving (12) when the driving angular frequency ω_d lies inside the stop gap, namely,

$$\omega_d \in \,]1, \omega_0[\,, \tag{16}$$

for which we shall demonstrate that above a threshold amplitude a_s of the boundary driving (12), energy is transmitted through the medium by means of *slow-light solitons*.

III. NONLINEAR SUPRATRANSMISSION PREDICTION

In order to predict the existence of a threshold of energy transmission by nonlinear process, we consider the nonlinear Schrödinger limit of the MB system (1), with vanishing dissipation, derived in [32]. With the electric field (4) we define carrier and envelope components at first order (see [32] for details) by

$$E(z,t) \simeq \psi(z,t) e^{i(\omega t - kz)} + \text{c.c.} + \cdots, \tag{17}$$

where the envelope ψ is a *slowly varying* function of z and t, and where ω is related to k by the linear dispersion relation (14). The resulting equation reads

$$-i\lambda(\psi_t - v_g \psi_z) + \mu \psi_{zz} + \alpha \rho |\psi|^2 \psi = 0, \tag{18}$$

for the following definitions:

$$v_g = \frac{d\omega}{dk} = k\omega \frac{1 - \omega^2}{k^2 - \omega^4}, \tag{19}$$

$$\lambda = \frac{2}{\omega}\frac{1-\omega^2}{1+\omega^2}\frac{k^2-\omega^4}{\omega^2-k^2}, \tag{20}$$

$$\mu = \omega^2\frac{(1-\omega^2)^2}{1+\omega^2}\frac{3k^2+\omega^4}{(\omega^4-k^2)^2}, \tag{21}$$

$$\rho = \frac{3+\omega^2}{2(1+\omega^2)}. \tag{22}$$

From the solution $\psi(z,t)$ of Eq. (18), the physical (dimensionless) quantities are obtained by Eq. (17) for the electric field and by

$$P(z,t) \simeq \frac{\alpha}{1-\omega^2}\psi(z,t)e^{i(\omega t-kz)} + \text{c.c.}, \tag{23}$$

$$N(z,t) \simeq -1 + \frac{\alpha}{1-\omega^2}\frac{1+\omega^2}{1-\omega^2}\psi(z,t)\bar{\psi}(z,t) + \frac{1}{2}\frac{\alpha}{1-\omega^2}(\psi(z,t)^2 e^{2i(\omega t-kz)} + \text{c.c.}). \tag{24}$$

Note the presence of the second harmonic in the population inversion $N(z,t)$, fundamental to interpret the nonlinear propagation of a slow-light gap soliton.

In the present situation, the electric field at the boundary $z=0$ has its frequency inside the stop gap, close to the upper band edge, namely,

$$\omega_d = \omega_0 - \nu, \quad \frac{\nu}{\omega_0} \ll 1. \tag{25}$$

Consequently the carrier wave frequency ω is precisely the upper band edge ω_0 and the envelope equation (18) simplifies to

$$-i\omega_0\psi_t + \frac{\omega_0^2-1}{2\omega_0^2}\psi_{zz} + \frac{1}{4}(\omega_0^2+3)|\psi|^2\psi = 0, \tag{26}$$

by evaluating the coefficients (19)–(22) at $k=0$ and $\omega=\omega_0$. Note in particular that v_g vanishes which allows the boundary value problem on $z\in[0,L]$ for the MB system to map to a boundary value problem on $[0,L]$ for the above nonlinear Schrödinger equation, namely,

$$\psi(0,t) = \frac{a}{2}e^{-i\nu t}, \quad \psi_z(L,t) = 0, \quad \nu = \omega_0 - \omega_d. \tag{27}$$

For a long length medium ($L\to\infty$), the solution to that boundary value problem reads as the stationary soliton solution to Eq. (26),

$$z \geq 0: \psi(z,t) = \frac{Ae^{-i\nu t}}{\cosh\kappa(z-z_0)}, \tag{28}$$

$$\kappa^2 = \frac{2\nu\omega_0^3}{\omega_0^2-1}, \quad A^2 = \frac{8\nu\omega_0}{\omega_0^2+3}, \tag{29}$$

where the amplitude a determines the center position z_0 by the matching requirement

$$\frac{a}{2} = \frac{A}{\cosh\kappa z_0}. \tag{30}$$

There exists a real-valued solution z_0 to that equation as far as $a\leq 2A$, which furnishes the sought threshold $a_s=2A$ given thus by

$$a_s^2 = 32\frac{(\omega_0-\omega_d)\omega_0}{\omega_0^2+3}. \tag{31}$$

We conclude that the boundary value (12) for the electric field component of angular frequency ω_d and amplitude a produces an evanescent field in the two-level medium as long as $a<a_s$, a value which is completely determined by the stop gap edge ω_0 and the applied frequency ω_d. Above this value, namely for $a>a_s$, we observe an instability (described in the last section) that produces a solitonlike excitation which then propagates away from the boundary.

IV. NUMERICAL SIMULATIONS

The above prediction is now compared to numerical simulations of the MB model (8) under initial-boundary values (11)–(13). Some precaution must be taken to settle the cw boundary driving equation (12) which is not compatible with vanishing initial data. The numerical simulation is thus started at zero amplitude at $t_0=-100$ followed by a transient sequence where it is slowly increased to the value a reached at $t=0$. We thus set the initial data for all z as

$$t=t_0: E=P=0, \quad E_t=P_t=0, \quad N=-1, \tag{32}$$

and the boundary values for all times as

$$E(0,t) = a(t)\sin(\omega_d t), \quad E_z(L,t) = 0,$$

$$a(t) = \frac{a}{2}[\tanh(0.05(t+40)) - \tanh(0.05(t-200))], \tag{33}$$

where the driving is stopped after $t=200$ to avoid creation of more than one soliton. The following numerical simulations are performed without damping: $\gamma_1=\gamma_2=\gamma=0$.

Typical results of a numerical simulation are displayed on Fig. 3 at driving angular frequency $\omega_d=1.4$ when the gap edge lies at $\omega_0=1.414$ (for a coupling constant $\alpha=1$). We compute in particular the (normalized) value of the energy density stored in the polarization (units $w_0=N_0\hbar\Omega/2$)

$$W(z,t) = -\frac{1}{2}P(z,t)E(z,t), \tag{34}$$

at a given time (here $t=300$) for a given driving amplitude close to the predicted threshold. Thus energy does propagate inside the medium above a threshold amplitude which allows one to build the bifurcation diagram when varying the driving frequency and to compare to the theoretical prediction (31). This results in Fig. 4, which shows agreement when the driving frequency becomes close to the gap edge, accordingly with the fact that our prediction is based on the NLS limit model (26) accurate only when the condition (25) holds.

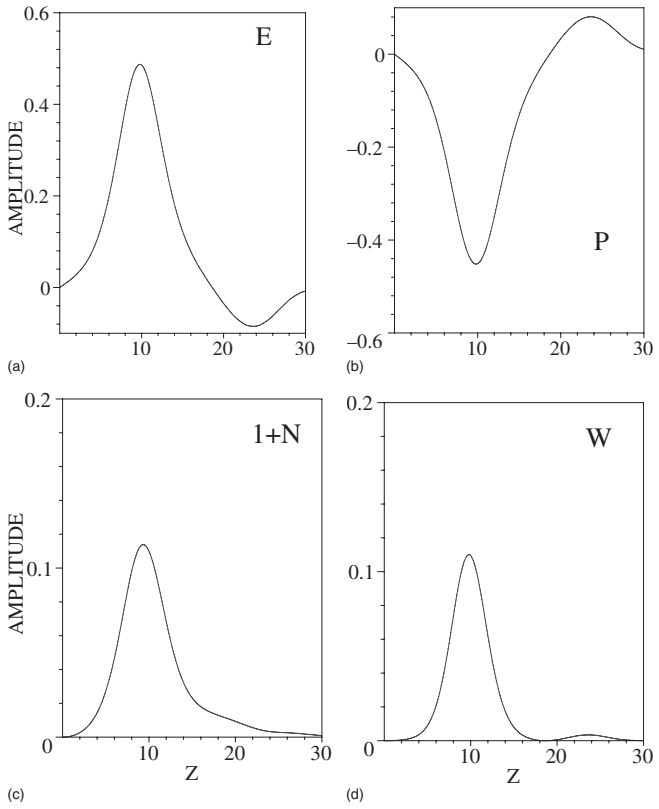

FIG. 3. Typical numerical solution of Eq. (8): dimensionless plots of the electric field (E), the polarization (P), the density of excited atoms ($1+N$), and the energy density (W) as functions of z (horizontal axis) at time $t=300$ for the boundary values (33) with frequency $\omega_d=1.4$ and amplitude $a=0.32$. The same simulation at $a=0.28$ does not show any energy transmission.

An intensity plot of the numerical solution of Eq. (8) is shown for illustration of nonlinear supratransmission on Fig. 5 with boundary driving frequency 1.4 and amplitude 0.35. The generated breather moves at velocity 0.10. The external driving actually started about $t=0$, according to Eq. (33), and the first breather is generated about $t=150$, a time necessary to allow for the instability to develop. We may remark on the plots of Fig. 5 the periodic marks appearing on the pulse location. These are not an effect of the numerical code but the manifestation of the way light propagates nonlinearly in the medium, a fundamental effect now discussed.

V. PERIODIC ENERGY EXCHANGE

It is quite interesting indeed to understand how light actually propagates in the medium at a velocity less than the light velocity. It occurs by a periodic permanent energy exchange between *polarization* and *population*, namely between the electromagnetic polarization energy density (W) and the density of excited state ($1+N$). This process is represented by the above mentioned periodic oscillations of the amplitudes in Fig. 5 which are displayed differently in Fig. 6. There, one sees the polarization energy (plot of W) and the population density of excited state (plot of $1+N$) exchanging amplitude periodically, with a period value measured on Fig. 5 to be $T=2.27$ and checked by the plots of Fig. 6.

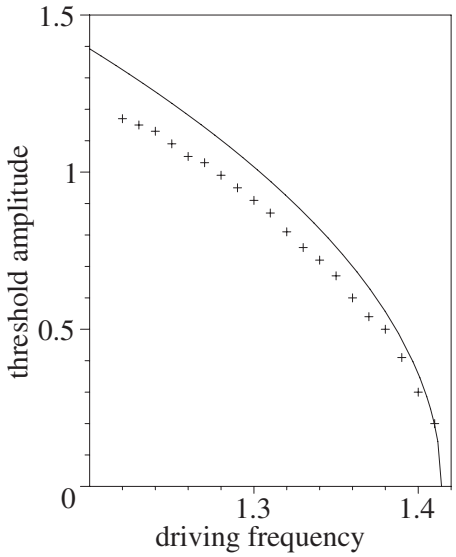

FIG. 4. Bifurcation diagram representing the threshold amplitude (vertical axis) in terms of the driving angular frequency (horizontal axis). The full line is the prediction (31) while the crosses are the thresholds obtained by numerical simulation of the MB model (8).

The oscillation process that slows down light is now understood by calling to the NLS limit for which the propagating pulse of the Maxwell-Bloch system can be approximated by expressions (17), (23), and (24), written now for $\omega=\omega_0$, which eventually provide

$$W \simeq |\psi|^2 + \Re(\psi^2 e^{2i\omega_0 t}), \tag{35}$$

$$1 + N \simeq \left(1 + \frac{2}{\alpha}\right)|\psi|^2 - \Re(\psi^2 e^{2i\omega_0 t}), \tag{36}$$

where we have used the definition $\alpha=1-\omega_0^2$, and where $\Re$

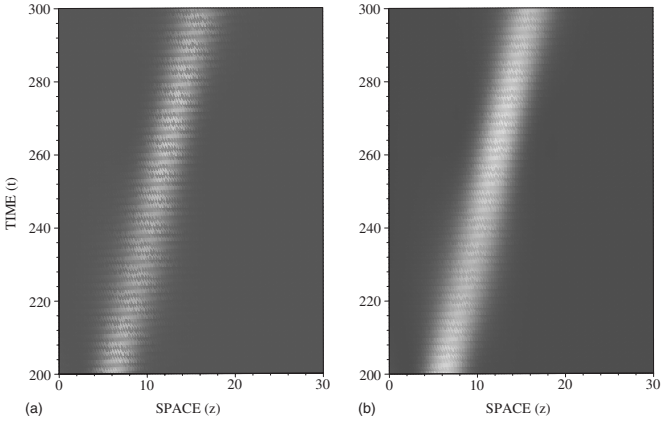

FIG. 5. Dimensionless intensity plot of the polarization energy density W (left) and the density of excited atoms $1+N$, (right) for driving parameters $a=0.35$, $\omega_d=1.4$. The vertical axis is the time t, and the horizontal axis is the position z in the medium. The modulation of the intensities is measured to have a period of 2.27 (normalized time).

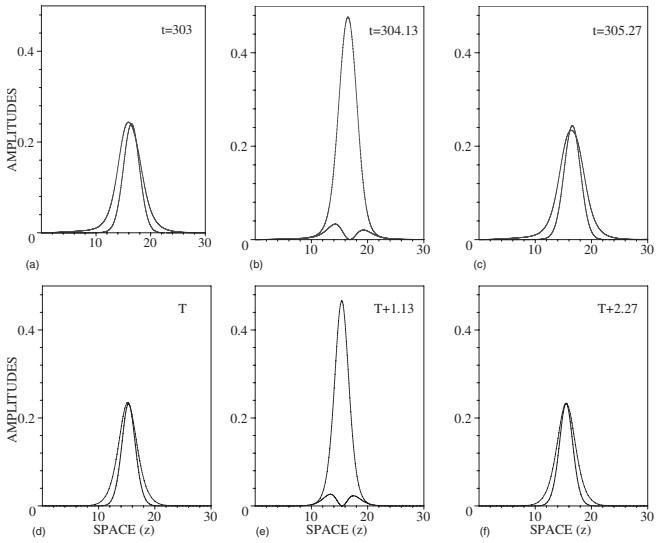

FIG. 6. Propagation of light inside the two-level medium proceeding by continuous periodic exchange of energy between polarization and population of the excited level. The dashed line is $1+N(z,t)$, the full line is $W(z,t)$, both plotted as functions of z (dimensionless quantities) at three different times as indicated. Top: results of numerical simulations of MB taken from Fig. 5. Bottom: fit obtained by the solution of NLS according to expressions (35) and (36).

means *real part*. Consequently, those two quantities possess a permanent component over which an oscillation having the period of $\psi^2 e^{2i\omega_0 t}$ is superposed with a phase opposition between W and $1+N$, as apparent on Fig. 6.

We may compare now the NLS model with numerical simulations. The soliton solution to Eq. (26) writes (up to a translation of time and space)

$$\psi(z,t) = \frac{Be^{i(\beta z-\mu t)}}{\cosh[\kappa(z-vt)]}, \quad \beta = v\frac{\omega_0^3}{1-\omega_0^2},$$

$$\kappa^2 = \frac{B^2}{4}\omega_0^2\frac{\omega_0^2+3}{\omega_0^2-1}, \quad \mu = (\beta^2-\kappa^2)\frac{1-\omega_0^2}{2\omega_0^3}. \tag{37}$$

The fit is obtained by measuring on the numerical simulations of MB the two determining parameters: the velocity v and the amplitude B. Using the simulations of Fig. 5, we obtain $v=0.10$ and $B=0.346$, which provide through expression (35) and (36) the plots of the second line in Fig. 6 at some convenient time T. As a consequence, the theoretical value of the period of the oscillations can be evaluated as $\pi/(\omega_0-\mu)$ and we obtain the value 2.28.

Note that the above moving soliton should not be confused with the expression of the boundary *stationary soliton tail* (28) which results from the boundary value imposed in $z=0$ and which holds only when its amplitude is below the threshold.

VI. GENERATING INSTABILITY

To complete the picture of the soliton generation process, we briefly describe here the linear stability analysis that shows the mechanism by which an instability grows when the driving amplitude exceeds the threshold value. To that end we consider the approximate model (26), namely

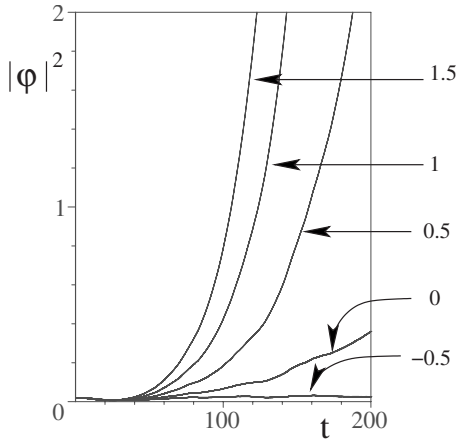

FIG. 7. Dimensionless amplitudes $|\varphi(z,t)|^2$ at fixed $z=5$ on a line $L=20$ obtained by solving Eq. (41) for a constant initial condition plotted as a function of time t for different values of the position z_0 as indicated.

$$-i\psi_t + \frac{\omega_0^2-1}{2\omega_0^3}\psi_{zz} + \frac{\omega_0^2+3}{4\omega_0}|\psi|^2\psi = 0, \tag{38}$$

on the finite interval $z\in[0,L]$ and look at the evolution of the deformations of the static soliton solution stuck on the boundary $z=0$ and centered in $z=z_0$ according to expression (28). We thus set

$$\psi(z,t) = [S(z-z_0)+\epsilon\varphi(z,t)]e^{-i\nu t}, \tag{39}$$

$$S(z-z_0) = \frac{A}{\cosh\kappa(z-z_0)}, \tag{40}$$

where the parameters A and κ are given from $\nu=\omega_0-\omega_d$ by expressions (29).

At first order in ϵ, the linear equation for the perturbation φ then reads

$$-i\varphi_t + \frac{\omega_0^2-1}{2\omega_0^3}\varphi_{zz} + \frac{\omega_0^2+3}{4\omega_0}(2\varphi+\bar{\varphi})S^2 = \nu\varphi. \tag{41}$$

It is a Schrödinger scattering problem for the vector $(\varphi,\bar{\varphi})$, of energy ν, on the semiaxis $z>0$ in the confining potential $-S^2(z-z_0)$. At this point, one would like to display explicit solutions to Eq. (41) and demonstrate that when the position z_0 becomes positive, an eigenvalue becomes complex and the solution φ grows exponentially, as done in [25]. Although we do not have such solutions, the instability of the linear perturbation is easily demonstrated by numerical simulations of Eq. (41) when varying the center position z_0 from negative values (stable) to positive ones (unstable) as displayed on Fig. 7.

Then for negative values of z_0, which means for driving amplitudes less than the threshold value, the linear perturbation does not grow and the solution is stable. For positive z_0 the linear perturbation grows exponentially (at $z_0=0$ it grows

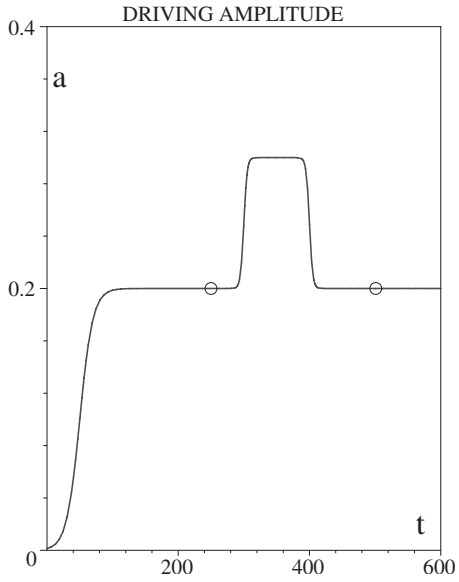

FIG. 8. Dimensionless time variation of the amplitude a in the boundary value (12). The two points indicate the time values at which the solution is plotted on Fig. 9.

linearly), which shows the instability mechanism for soliton generation. It is worth noting that this instability is a direct consequence of the *boundary value* nature of the problem to be solved. Indeed, the same situation on the infinite line would evidently be stable: for $z \in \mathbb{R}$, the invariance by translation along z guarantees that the behavior of the perturbation about the initial pulse centered in z_0 cannot depend on z_0.

VII. OPTICAL BISTABILITY

Another essentially nonlinear property is the bistability that manifests in the solution behavior that can have different outputs for a given input and different *history*. As an example we solve the system (8), on a short length $L=4$, for initial-boundary value data as Eqs. (11) and (12), where the amplitude a varies in time according to the plot of Fig. 8.

In order to allow stabilization of the solution we include small damping in the model by using the following parameters

$$\gamma = 0.01, \quad \gamma_1 = 0.01, \quad \gamma_2 = 0.01, \tag{42}$$

which means finite dephasing times T_1 and T_2 together with nonzero field attenuation factor $\mathcal{A}$. The result of numerical simulations (still with a driving frequency $\omega_d = 1.4$) is displayed in Fig. 9, where the state of the system, after the perturbation of the driving amplitude a within $t \in [300,400]$, is radically different from the state before.

Again, here this process can be understood by using the NLS limit model (26) which is now solved for periodic solutions as follows. Let us seek a stationary solution of Eq. (26) submitted to the boundary value problem (27) under the form

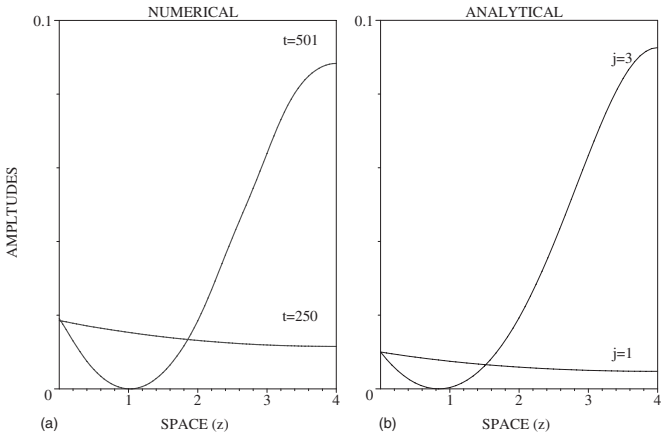

FIG. 9. Dimensionless polarization energy density W, plotted as a function of (dimensionless) space z. Left: obtained form the solution of Eq. (8) for a boundary driving equation (12), where the amplitude a varies according to Fig. 8 for two different values of time as indicated. Right: plot of the analytical expression (59) of $W(z,t)$, at some convenient value of time t, for $j=3$ and $j=1$.

$$\Psi(z,t) = \phi(\zeta)e^{-i\nu t}, \quad \zeta = z\omega_0\sqrt{\frac{\omega_0^2+3}{2(\omega_0^2-1)}}, \tag{43}$$

to obtain for the real-valued amplitude $\phi(\zeta)$

$$\frac{\partial^2\phi}{\partial\zeta^2} + \phi^3 = g\phi, \quad g = \frac{4\nu\omega_0}{\omega_0^2+3}, \tag{44}$$

$$\phi(0) = \frac{a}{2}, \quad \left.\frac{\partial\phi}{\partial\zeta}\right|_{z=L} = 0. \tag{45}$$

Such an equation possess a set of explicit solutions in terms of Jacobi elliptic function which we may write [33]

$$\phi_1(\zeta) = A_1 cn[\kappa_1(\zeta - D), \mu_1], \tag{46}$$

$$\phi_2(\zeta) = A_2 dn[\kappa_2(\zeta - D), \mu_2], \tag{47}$$

$$\phi_3(\zeta) = A_3 dn^{-1}[\kappa_3(\zeta - D), \mu_3], \tag{48}$$

with the following parameter relations

$$\kappa_1^2 = \frac{g}{2\mu_1^2 - 1}, \quad A_1^2 = \frac{2g\mu_1^2}{2\mu_1^2 - 1}, \tag{49}$$

$$\kappa_2^2 = \frac{g}{2-\mu_2^2}, \quad A_2^2 = \frac{2g}{2-\mu_2^2}, \tag{50}$$

$$\kappa_3^2 = \frac{g}{2-\mu_3^2}, \quad A_3^2 = 2g\frac{1-\mu_3^2}{2-\mu_3^2}. \tag{51}$$

together with the scaled length

$$D = L\omega_0\sqrt{\frac{\omega_0^2+3}{2(\omega_0^2-1)}}. \tag{52}$$

By construction the ϕ_j's obey the free-end condition (45) and the A_j's are the output amplitudes $\phi_j(D)$.

As the parameters μ_j's are the moduli of the Jacobi elliptic functions, they all lie in $[0,1]$, consequently the output amplitudes belong to different ranges of values according to

$$\mu_1^2 = \frac{A_1^2}{2(A_1^2 - g)} \in [0,1] \Rightarrow A_1 \in [\sqrt{2g}, \infty], \tag{53}$$

$$\mu_2^2 = \frac{2A_2^2 - 2g}{A_2^2} \in [0,1] \Rightarrow A_2 \in [\sqrt{g}, \sqrt{2g}], \tag{54}$$

$$\mu_3^2 = \frac{2g - 2A_3^2}{2g - A_3^2} \in [0,1] \Rightarrow A_3 \in [0, \sqrt{g}]. \tag{55}$$

Now Eq. (45) fixes the input amplitude a, namely

$$\left(\frac{a}{2}\right)^2 = \frac{2g\mu_1^2}{2\mu_1^2 - 1} cn^2\left[\frac{D\sqrt{g}}{\sqrt{2\mu_1^2 - 1}}, \mu_1\right], \tag{56}$$

$$\left(\frac{a}{2}\right)^2 = \frac{2g}{2 - \mu_2^2} dn^2\left[\frac{D\sqrt{g}}{\sqrt{2 - \mu_2^2}}, \mu_2\right], \tag{57}$$

$$\left(\frac{a}{2}\right)^2 = 2g\frac{1 - \mu_3^2}{2 - \mu_3^2} dn^{-2}\left[\frac{D\sqrt{g}}{\sqrt{2 - \mu_3^2}}, \mu_3\right]. \tag{58}$$

Reporting hereabove the expressions (53)–(55) of the μ_j's eventually furnishes a in terms of the three A_j's in their respective intervals, it constitutes the bistability diagram.

In order to compare with the numerical solutions of the MB system (8), we solve equations (56)–(58) for the unknowns μ_j's with given amplitude a ($a=0.2$ for Fig. 9). It provides the values of the A_j's and thus the explicit expressions of the functions $\phi_j(\zeta)$ which are used to compute the polarization energy density W by expression (35). We obtain

$$W(z,t) = \phi_j^2[1 + \cos(2\omega_d t)], \tag{59}$$

an expression compared to the numerical simulations of the MB system on Fig. 9.

VIII. CONCLUSION

The analysis of the Maxwell-Bloch system in the situation where a cavity standing wave (linearly polarized) excites a two-level medium at one end have revealed the existence of a threshold of amplitude of cw irradiation (inside the forbidden band gap) above which nonlinear solitonlike pulses are generated in the medium.

These solitary excitations then propagate at a fraction of light velocity, by means of a periodic exchange between electromagnetic polarization energy and population inversion. Remarkably enough, this process is contained within the MB model and entirely results from nonlinearity that takes its origin in the coupling between field and two-level medium. It is fully understood in the NLS limit by keeping the second harmonic in the population inversion which shows once again that rigorous asymptotic limits are worth: a rough rotating wave approximation that would simply neglect higher harmonics would fail to explain the oscillations responsible for light slowing.

Although the MB system (8) does not possess known solitary wave solution, nonlinear supratransmission have succeeded to generate such structures, whose *numerical robustness* have been checked over long times ($t \geq 1200$) without dispersion. This is a common property of the nonlinear pulses generated by a boundary instability encountered in many nonintegrable systems, as nonlinear Klein-Gordon [30] or coupled mode equations in Bragg media [27].

In the case when the length of the medium is comparable with the typical solitary wave extension, the driven MB system locks to *periodic multistable solutions* as demonstrated by our numerical simulations. These states are understood by means of the Jacobi elliptic stationary solutions of the NLS limit with again a convincing agreement. As usual, such bistable systems are important to conceive sensitive detectors or digital amplifiers.

ACKNOWLEDGMENTS

This work was supported by CNRS contract 3073 GDR-PhoNoMi2 (*Photonique Nonlinéaire et Milieux Microstructurés*) with the CNRS.

[1] L. Brillouin, *Wave Propagation and Group Velocity* (Academic Press, New York, 1960).
[2] L. C. Allen and J. H. Eberly, *Optical Resonance and Two-Level Atoms* (Dover, New York, 1987).
[3] R. H. Pantell and H. E. Puthoff, *Fundamentals of Quantum Electronics* (Wiley, New York, 1969).
[4] S. L. Mac Call and E. L. Hahn, Phys. Rev. **183**, 457 (1969).
[5] A. I. Maimistov, A. M. Basharov, S. O. Elyutin, and Yu. M. Sklyarov, Phys. Rep. **191**, 11 (1990).
[6] G. L. Lamb, Jr., Phys. Rev. A **9**, 422 (1974).
[7] M. J. Ablowitz, D. J. Kaup, and A. C. Newell, J. Math. Phys. **15**, 1852 (1974).
[8] J. D. Gibbon, P. J. Caudrey, R. K. Bullough, and J. C. Eilbeck, Lett. Nuovo Cimento Soc. Ital. Fis. **8**, 775 (1973).
[9] I. R. Gabitov, V. E. Zakharov, and A. V. Mikhailov, Theor. Math. Phys. **63**, 328 (1985).
[10] M. Agrotis, N. M. Ercolani, S. A. Glasgow, and J. V. Moloney, Physica D **138**, 134 (2000).
[11] F. Hynne and R. K. Bullough, Philos. Trans. R. Soc. London, Ser. A **330**, 253 (1990).
[12] S. V. Branis, O. Martin, and J. L. Birman, Phys. Rev. Lett. **65**, 2638 (1990).
[13] B. I. Mantsyzov and R. N. Kuz'min, Sov. Phys. JETP **64**, 37 (1986).
[14] B. I. Mantsyzov, Phys. Rev. A **51**, 4939 (1995).
[15] B. I. Mantsyzov and R. A. Silnikov, J. Opt. Soc. Am. B **19**, 2203 (2002).
[16] B. I. Mantsyzov, JETP Lett. **82**, 253 (2005).

[17] W. Xiao, J. Zhou, and J. Prineas, Opt. Express **11**, 3277 (2003).
[18] I. V. Mel'nikov and J. S. Aitchison, Appl. Phys. Lett. **87**, 201111 (2005).
[19] A. E. Kozhekin and G. Kurizki, Phys. Rev. Lett. **74**, 5020 (1995).
[20] A. E. Kozhekin, G. Kurizki, and B. Malomed, Phys. Rev. Lett. **81**, 3647 (1998).
[21] N. Aközbek and S. John, Phys. Rev. E **58**, 3876 (1998).
[22] I. R. Gabitov, A. O. Korotkevitch, A. I. Maimistov, and J. B. McMahon, e-print arXiv:nlin.PS/0702049.
[23] P. J. Caudrey and J. C. Eilbeck, Phys. Lett. **62A**, 65 (1977).
[24] V. P. Kalosha and J. Hermann, Phys. Rev. Lett. **83**, 544 (1999).
[25] J. Leon, Phys. Lett. A **319**, 130 (2003).
[26] F. Geniet and J. Leon, Phys. Rev. Lett. **89**, 134102 (2002).
[27] J. Leon and A. Spire, Phys. Lett. A **327**, 474 (2004).
[28] R. Khomeriki, Phys. Rev. Lett. **92**, 063905 (2004).
[29] J. Leon, Phys. Rev. E **70**, 056604 (2004).
[30] F. Geniet and J. Leon, J. Phys.: Condens. Matter **15**, 2933 (2003).
[31] R. Khomeriki and J. Leon, Phys. Rev. E **71**, 056620 (2005).
[32] F. Ginovart and J. Leon, J. Phys. A **27**, 3955 (1994).
[33] P. F. Byrd and M. D. Friedman, *Handbook of Elliptic Integrals for Engineers and Physicists* (Springer, Berlin, 1954).